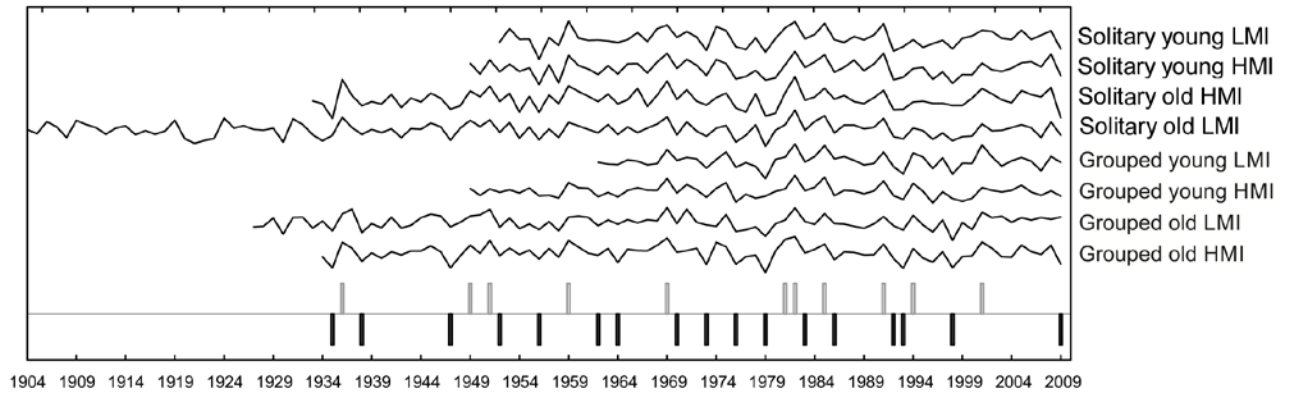


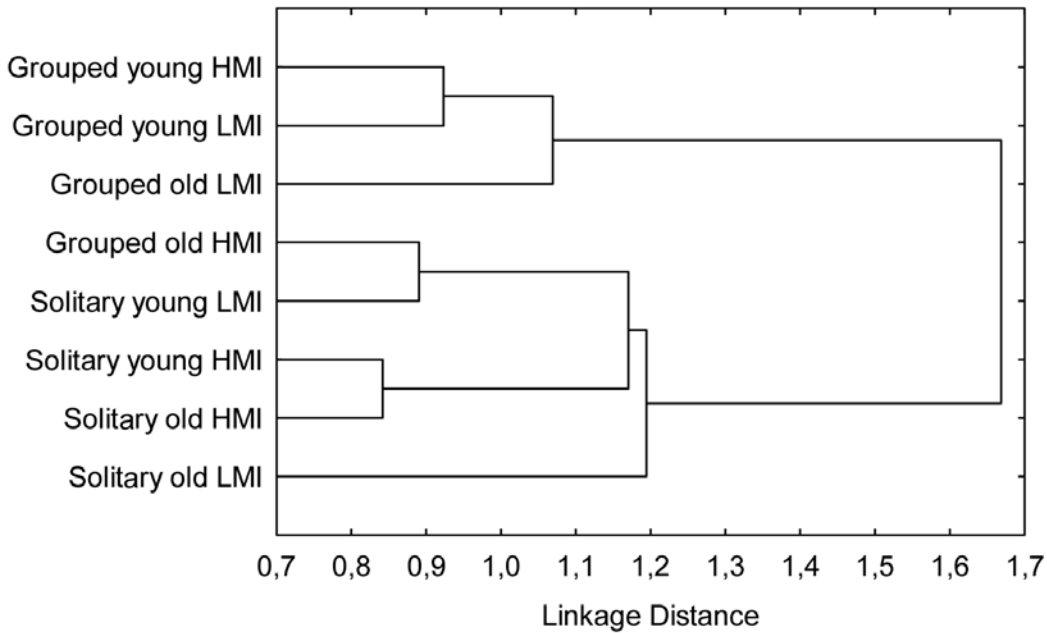
Doležal J., Lehečková E., Sohar K. & Altman J. (2016): Oak decline induced by mistletoe, competition and climate change: a case study from central Europe. – *Preslia* 88: 323–346.



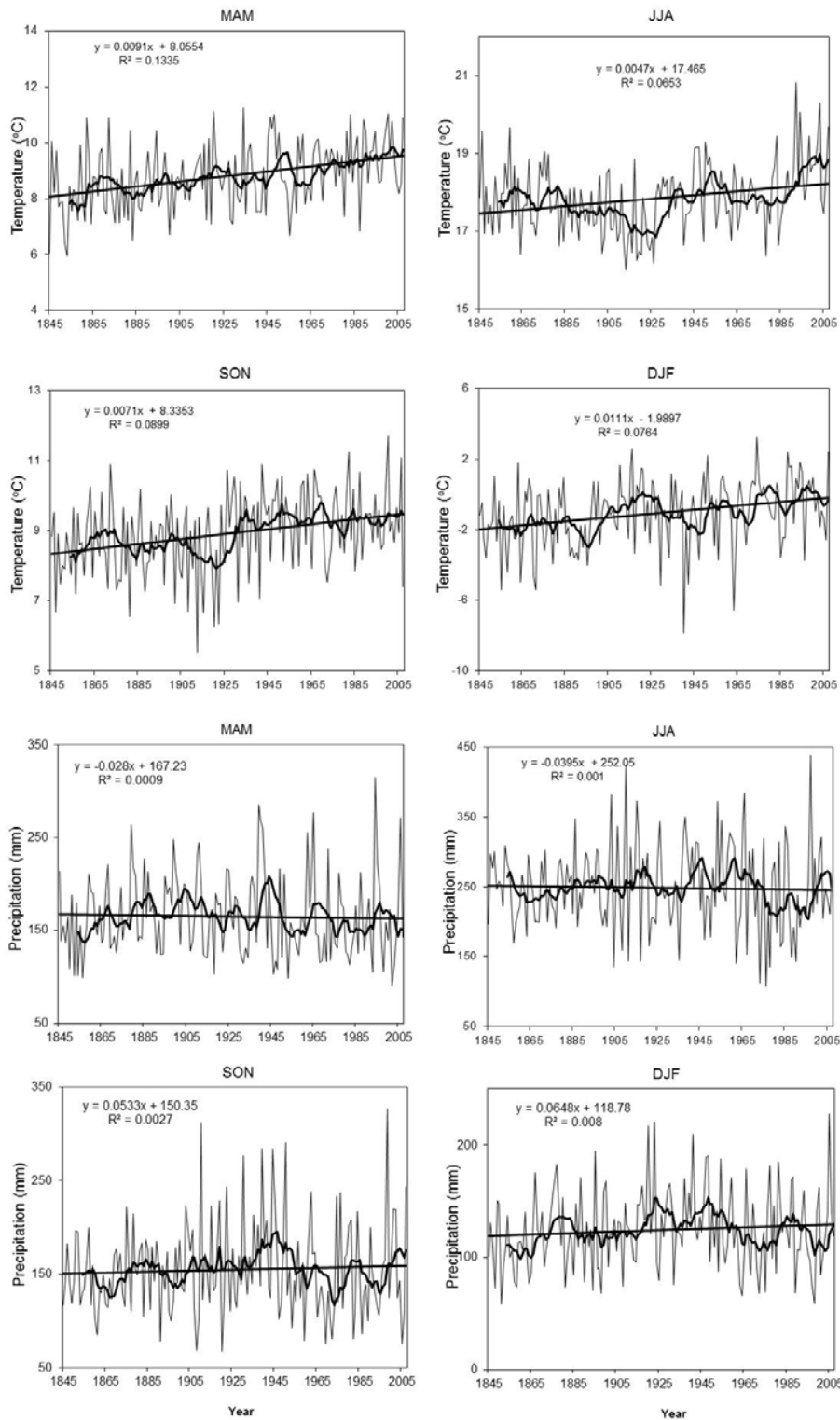
Electronic Appendix 1. The wooded grasslands of the National Nature Reserve of Čertoryje, the White Carpathians, Czech Republic, with scattered oaks (upper right) and small groves (bottom), where the tree-ring study was done. The whole complex is seen on the aerial photographs (from www.mapy.cz).



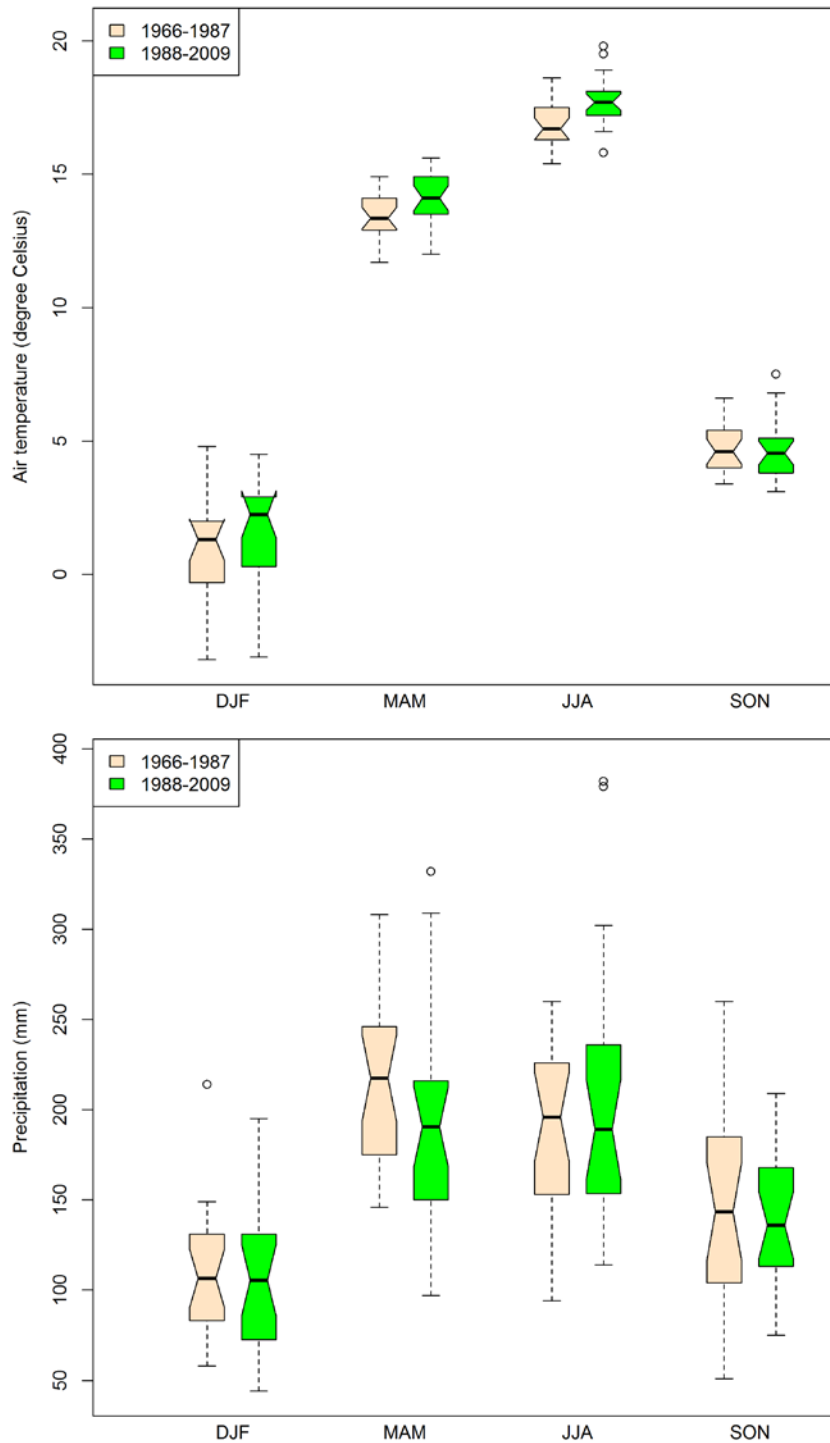
Electronic Appendix 2. The eight chronologies and pointer years common to most (and at least for 3) chronologies are displayed. Shaded and black columns represent positive and negative pointer years respectively. The pointer years were defined as those calendar years when at least 70% of the rings were at least 10% narrower or wider than the previous year. (Schweingruber 1996).



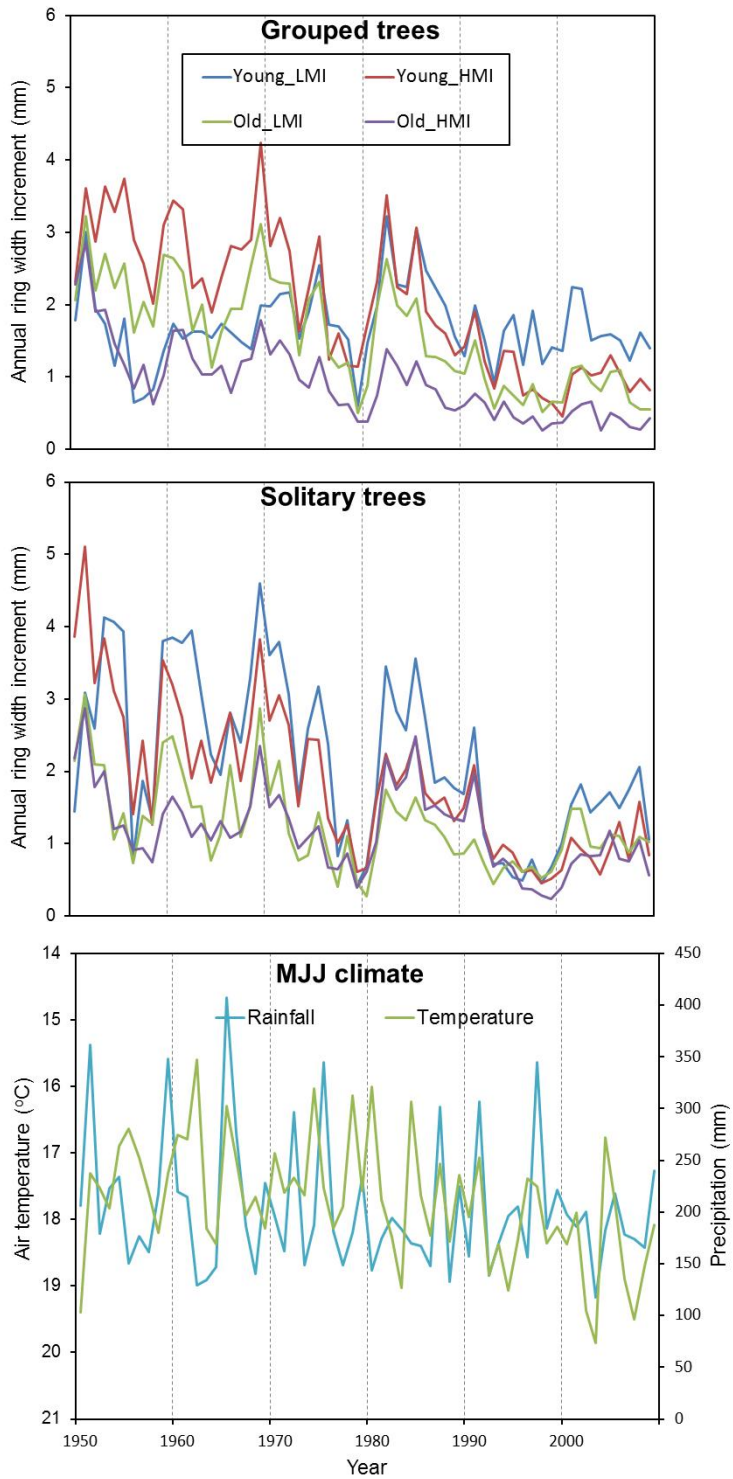
Electronic Appendix 3. Dendrogram presenting results of the hierarchical cluster analysis. Euclidian distances were calculated and chronologies were grouped together according to Ward's criterion.



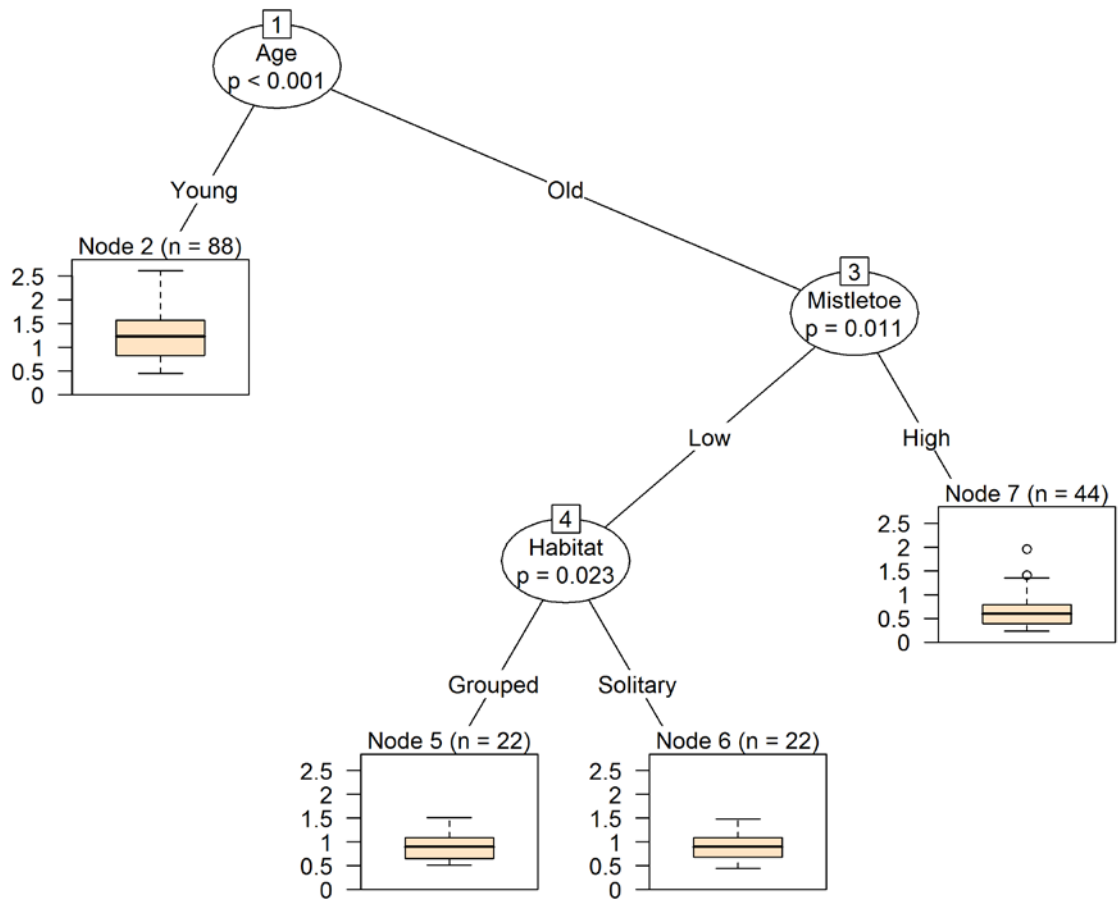
Electronic Appendix 4. The average temperature (a) and rainfall (b) recorded in the study area for the spring (MAM), summer (JJA), autumn (SON) and winter (DJF) periods, with smoothed values (10 year running mean) and fitted linear regression.



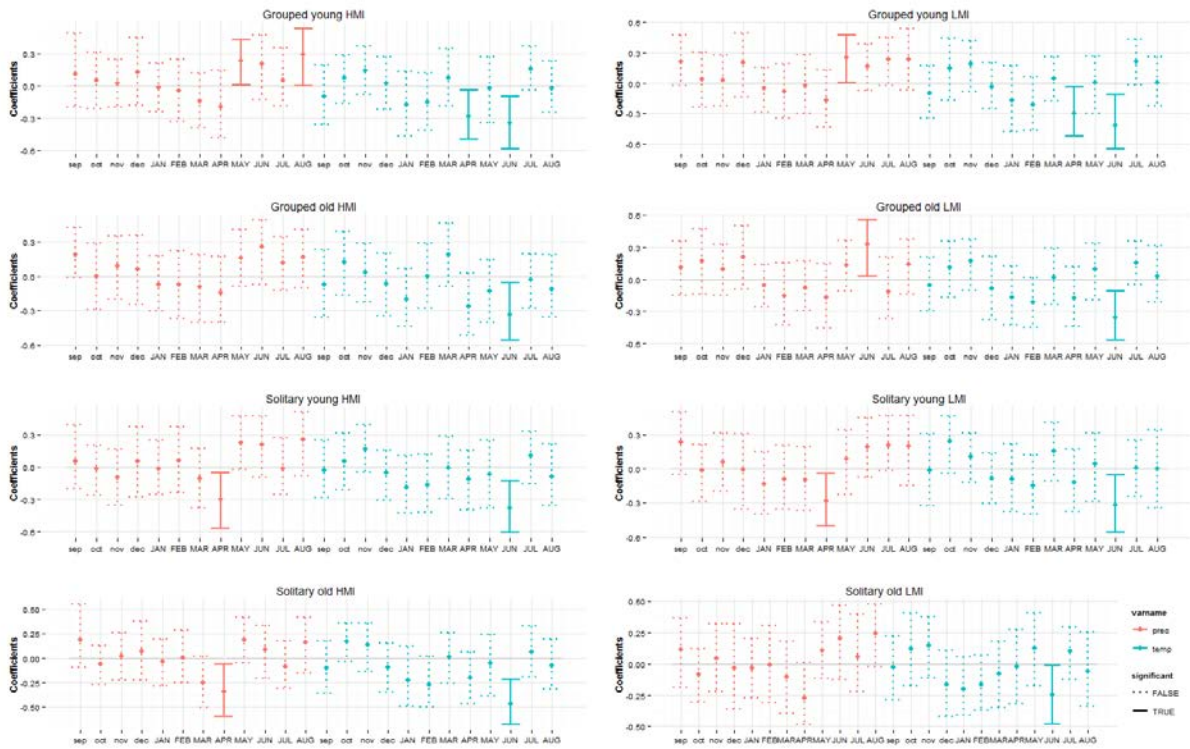
Electronic Appendix 5. Comparison of average temperature (a) and rainfall (b) recorded in the study area for the spring (MAM), summer (JJA), autumn (SON) and winter (DJF) periods for the 1966-1987 and 1988-2009.



Electronic Appendix 6. Differences in absolute ring width increments (AGR) between eight groups of oak trees in the period 1950-2009. Shown is also interannual variation in summer climate.

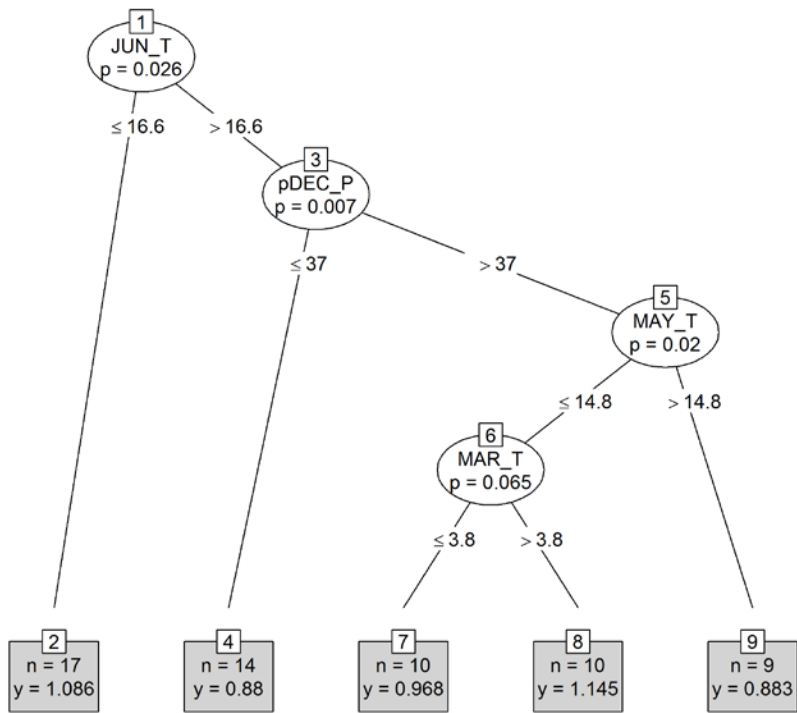


Electronic Appendix 7. The conditional inference trees showing a significant effect of all three factors (age, habitat, mistletoe) on AGR in the period 1966-1987.

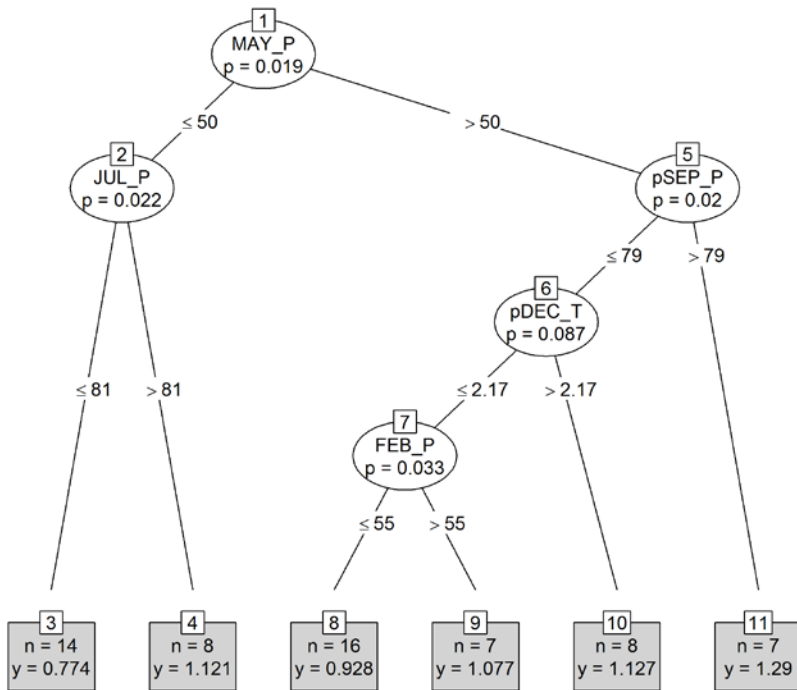


Electronic Appendix 8. Bootstrapped response function analysis between the eight oak latewood residual chronologies and climate data (precipitation, temperature) calculated over a 12-month window from September of previous year to current August for the overlap period 1962 – 2007. The abbreviated previous-year months are given in lowercase letters, the current-year ones in uppercase letters. Months with significant values are indicated by solid lines.

A. Grouped Young Oaks with High Mistletoe Infestation

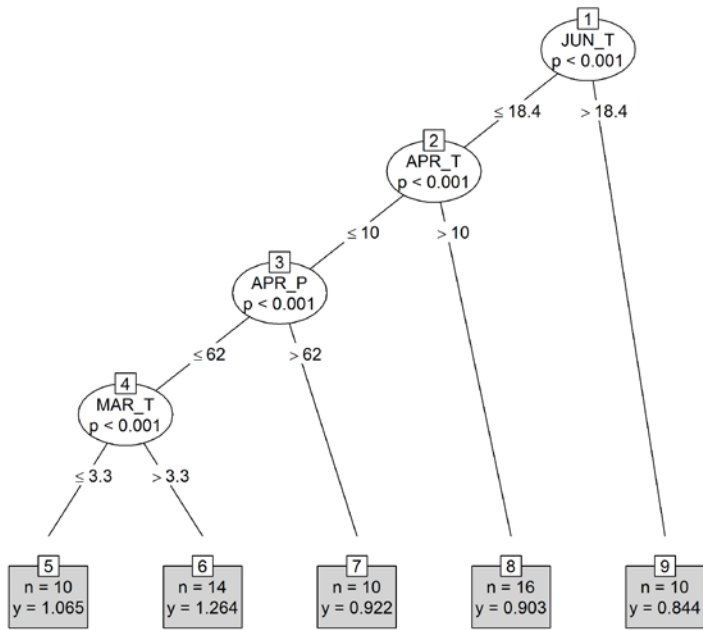


B. Grouped Young Oaks with Low Mistletoe Infestation

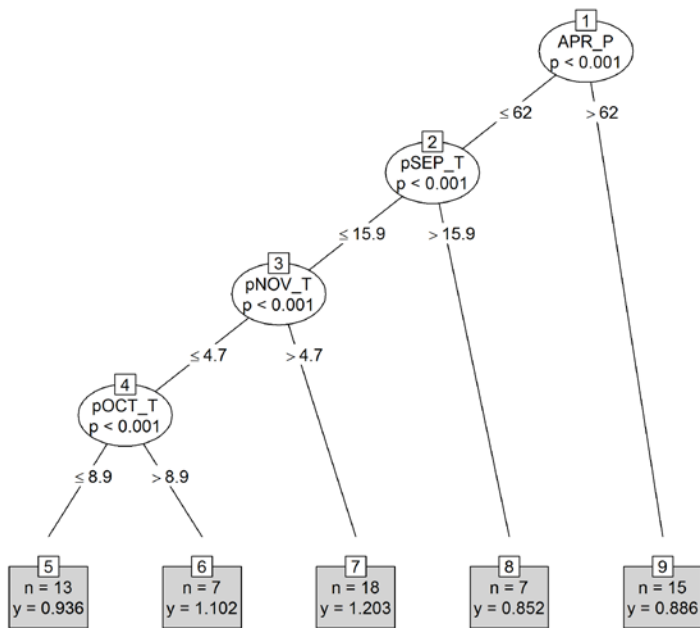


Electronic Appendix 9. Assessing nonlinear tree responses to climate using conditional inference trees for the grouped young oaks with two different levels of mistletoe infestation.

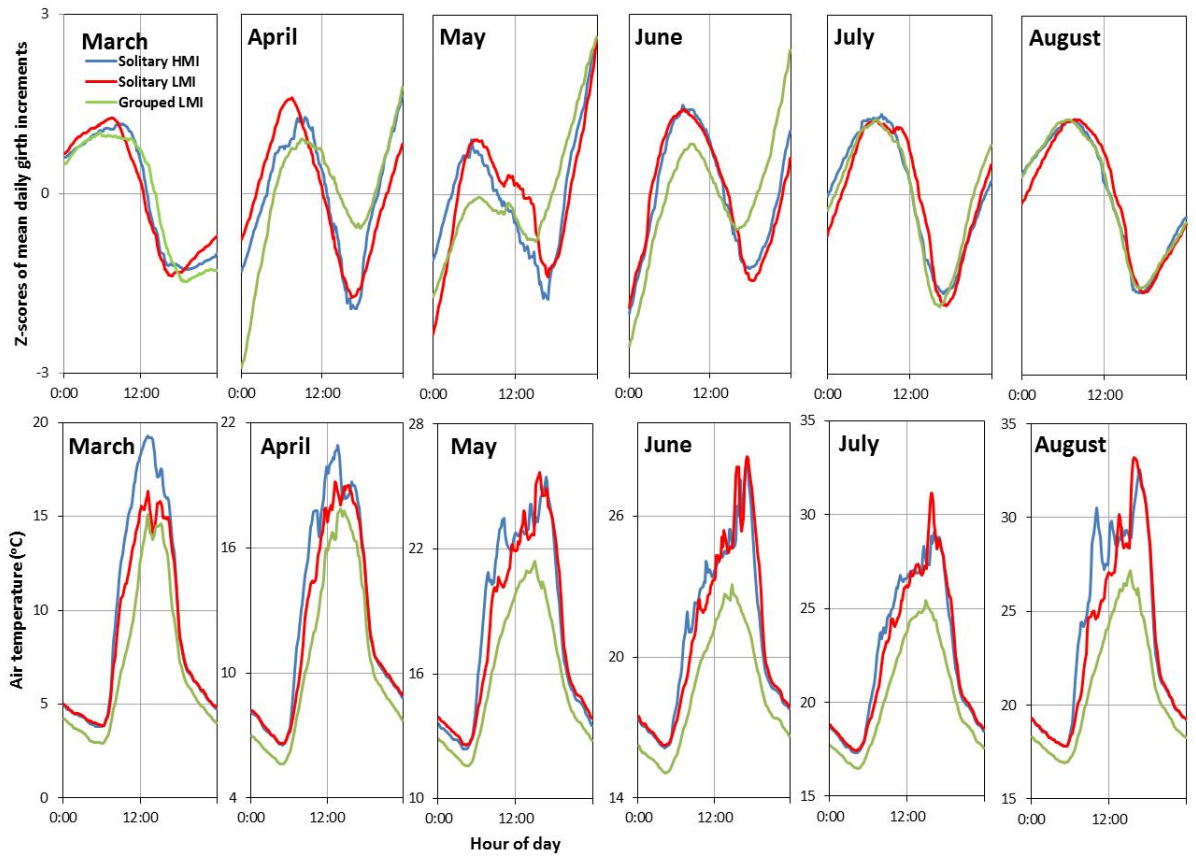
A. Grouped Old Oaks with High Mistletoe Infestation



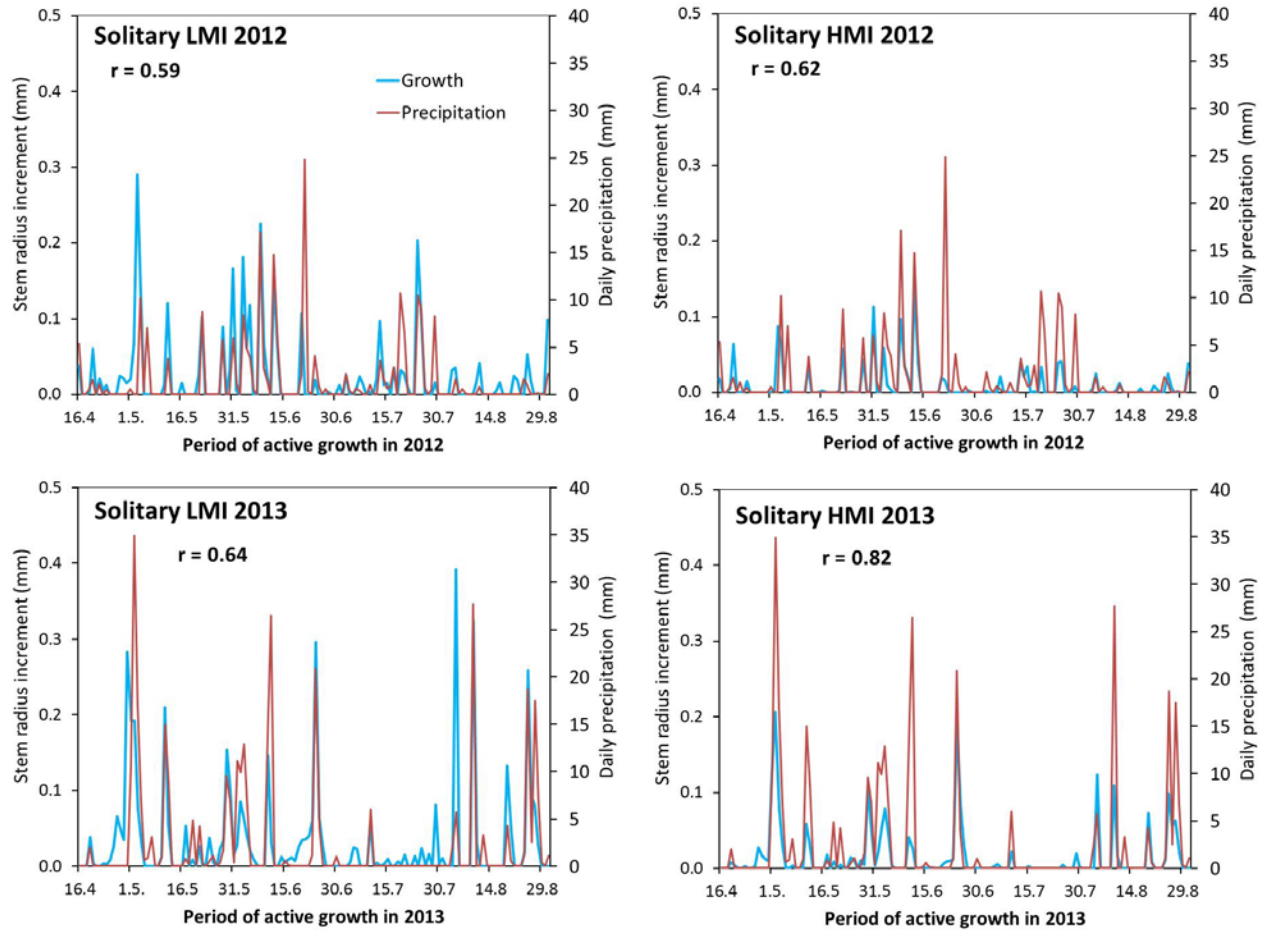
B. Grouped Old Oaks with Low Mistletoe Infestation



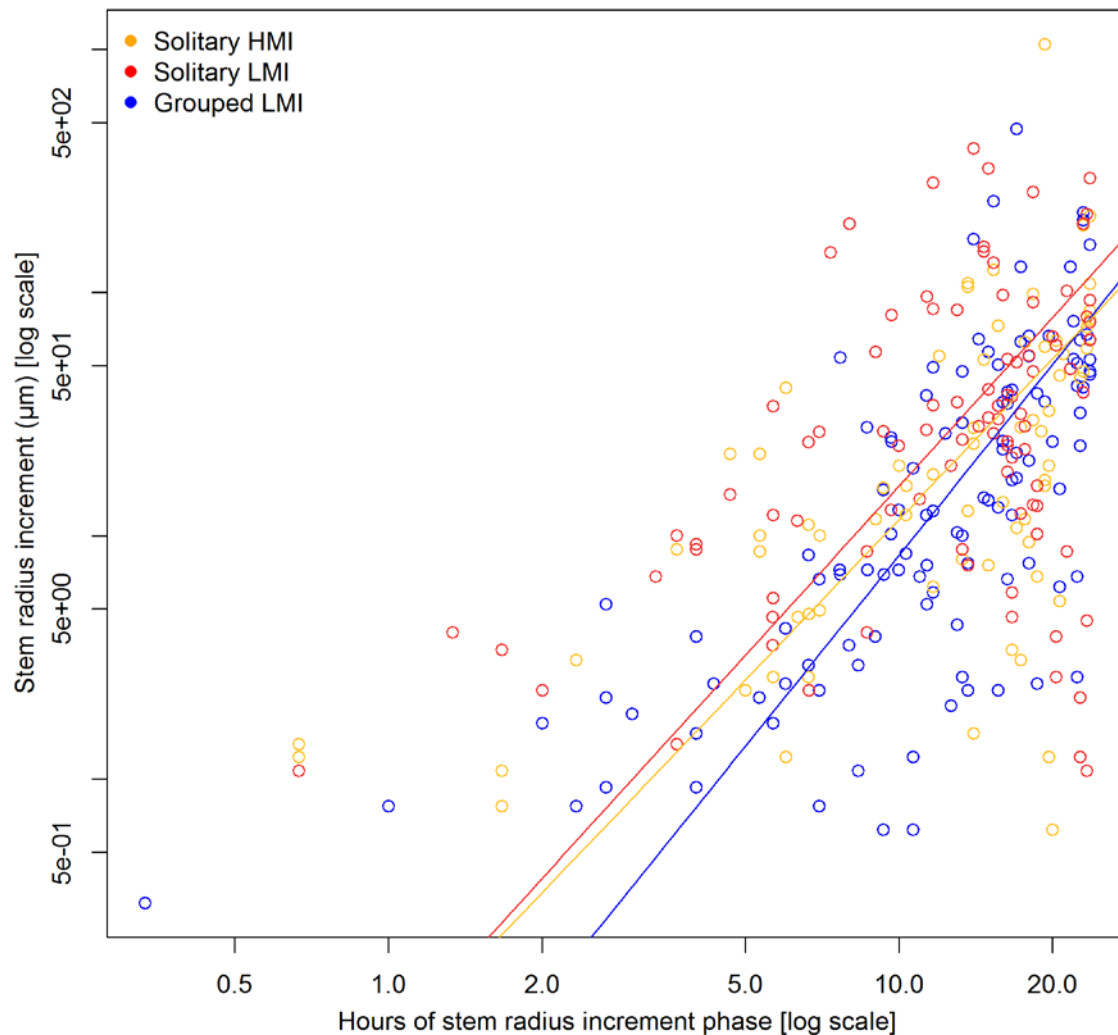
Electronic Appendix 10. Assessing nonlinear tree responses to climate using conditional inference trees for the grouped old oaks with two different levels of mistletoe infestation.



Electronic Appendix 11. Monthly mean circadian cycle of stem shrinking and swelling due to water loss and uptake during the March –August for the three tested oaks and the mean daily temperatures. Data consist of all dendrometer records averaged across two growing seasons (2012–2013).



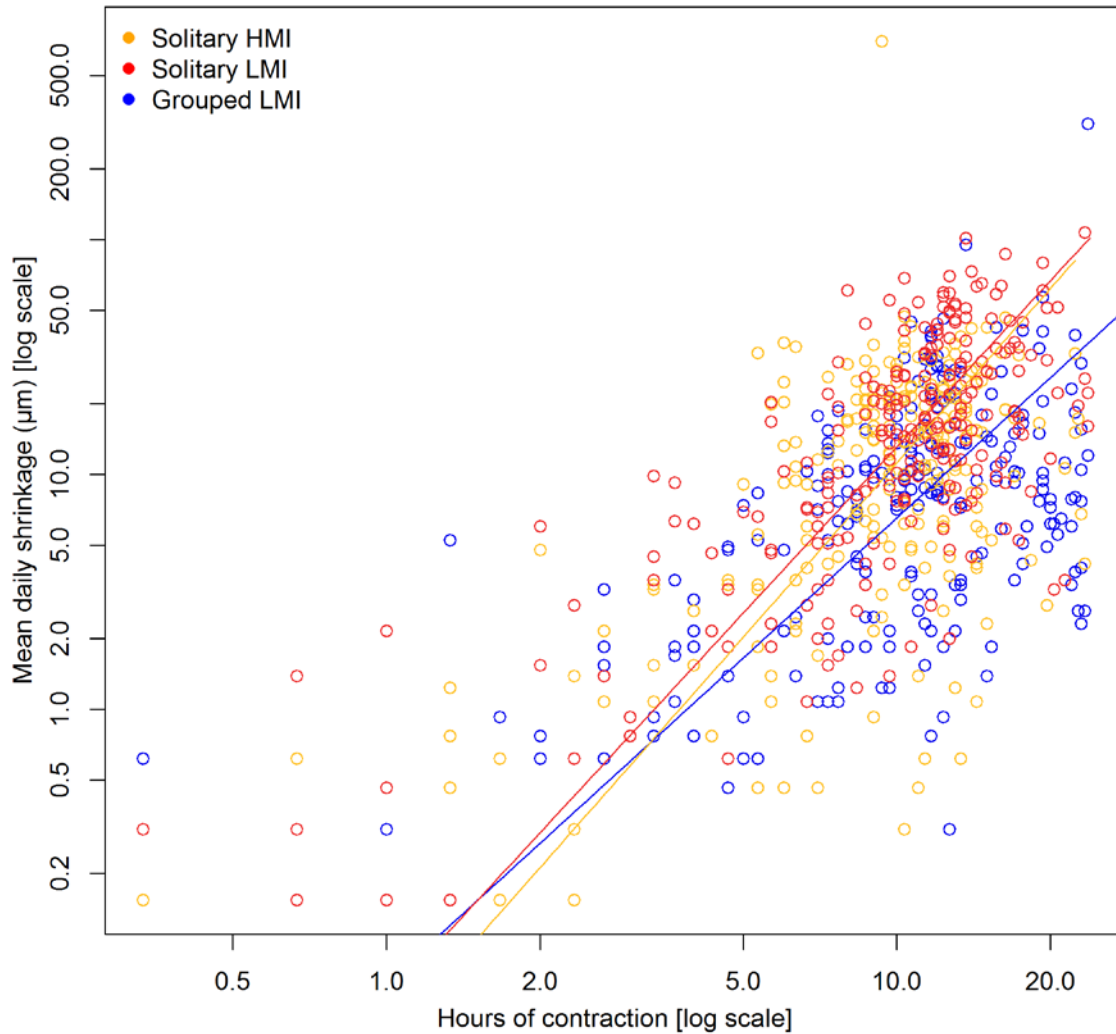
Electronic Appendix 12. The net daily increments are positively correlated with daily rainfall sum.



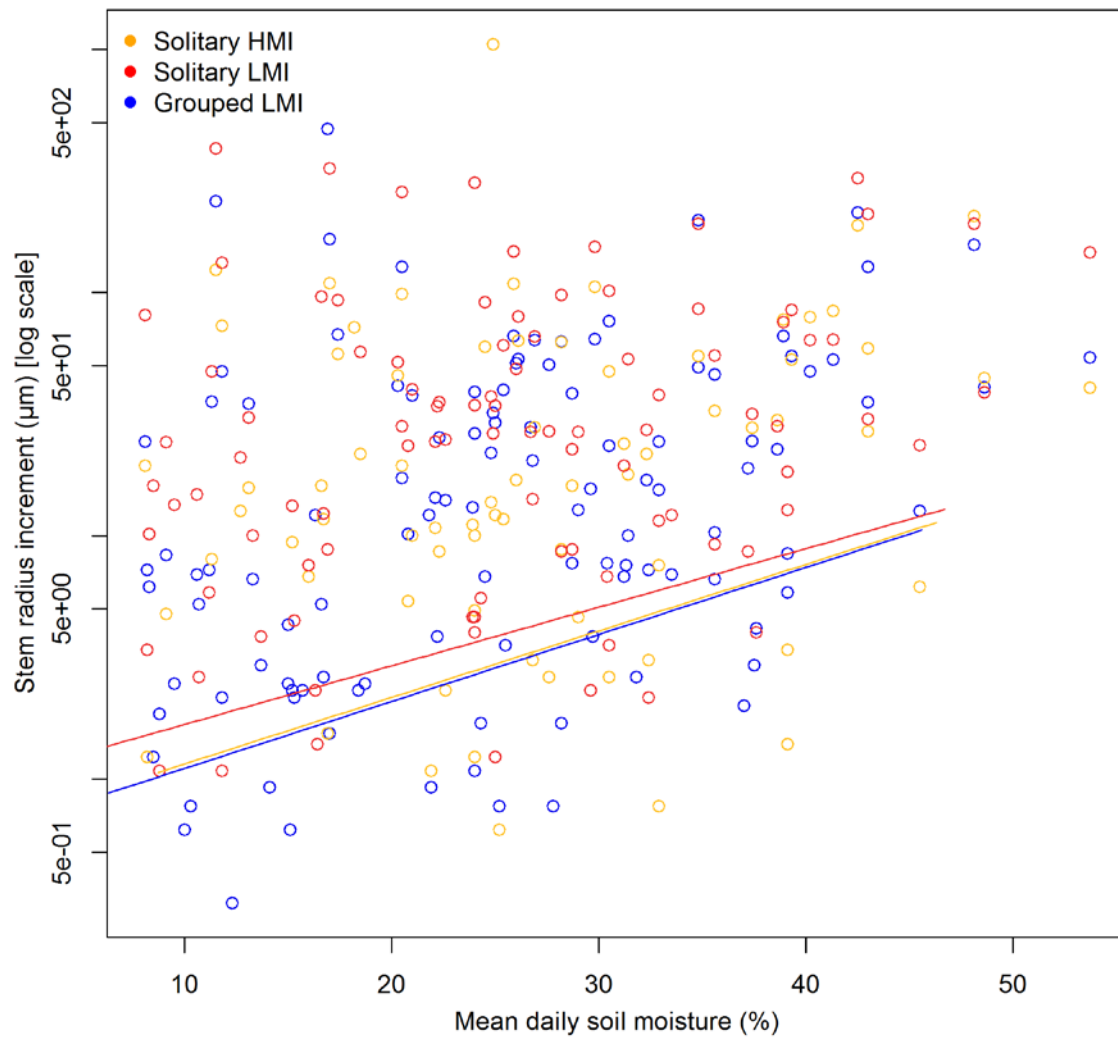
Electronic Appendix 13. Relationship between daily net stem radius increment (ΔR) and the duration (SRI) of the stem radius increment phase on a log-log scale for three oaks (solitary with low and high mistletoe infestation and grouped with low mistletoe infestation). The data were calculated from diurnal cycles in the period April–October 2013. ΔR was calculated when the stem radius exceeded the morning maximum until the subsequent maximum. Bivariate relationships were analyzed by fitting standardized major axes (SMA) (Warton et al. 2006; R Development Core Team 2009). SMA estimates of the line summarizing the relationship between two variables (i.e., the main axis along which two variables are correlated) are superior to ordinary linear regression estimates for these purposes, as residual variance is minimized in both X and Y dimensions, rather than in the Y dimension only.

All regressions were significant at $P < 0.01$. Solitary LMI: $\log(\Delta R) = -1.11 + 2.30\log(\text{SRI})$, $r^2 = 0.18$; Solitary HMI: $\log(\Delta R) = -1.12 + 2.19\log(\text{SRI})$, $r^2 = 0.35$; Grouped LMI: $\log(\Delta R) = -1.68 + 2.61\log(\text{SRI})$, $r^2 = 0.46$. There were nonsignificant pair-wise differences in the slopes of regression lines. Solitary LMI and grouped LMI differ in the intercept ($P = 0.005$).

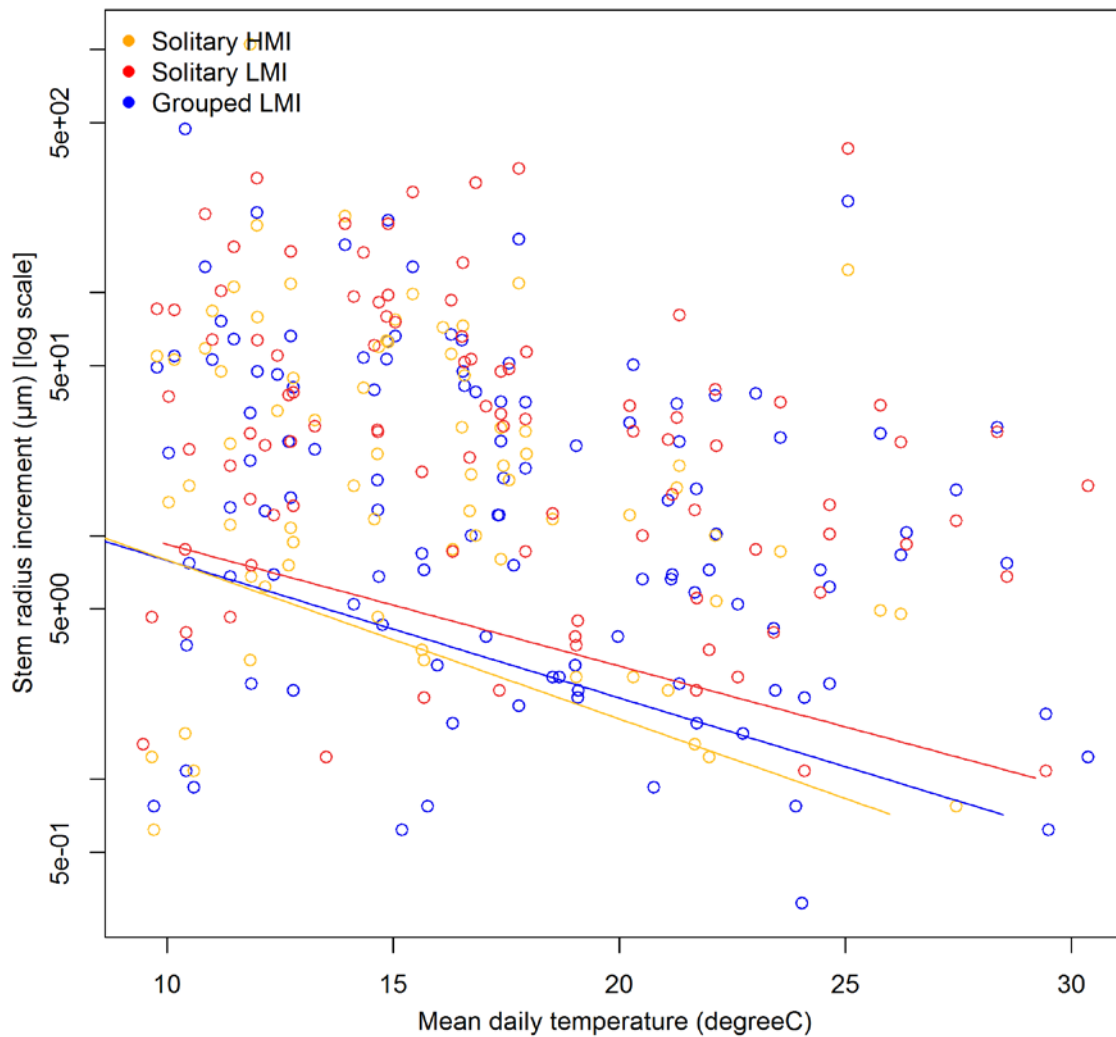
Warton D.I., Wright I.J., Falster D.S. & Westoby M. (2006): Bivariate line fitting methods for allometry. – *Biol Rev* 81: 259–291.



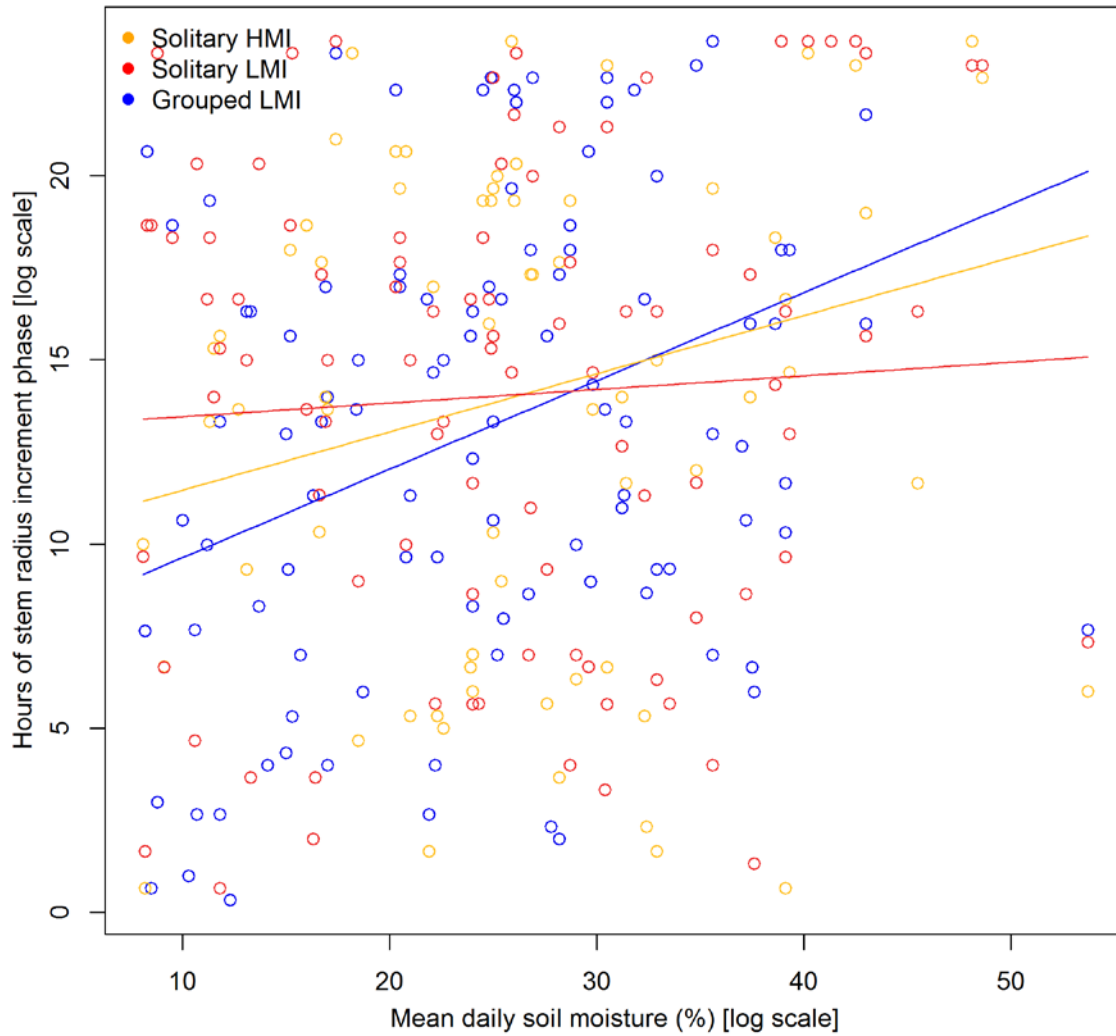
Electronic Appendix 14. Relationship between maximum daily shrinkage (MDS) and the duration of the contraction phase (DC) on a log-log scale for three oaks. The data were calculated from diurnal cycles in the period April–October 2013. MDS is the difference between the morning maximum and afternoon minimum of the circadian cycle. All regressions were significant at $P < 0.01$. Solitary LMI: $\log(\text{MDS}) = -1.23 + 2.35\log(\text{DC})$, $r^2 = 0.56$; Solitary HMI: $\log(\text{MDS}) = -1.41 + 2.46\log(\text{DC})$, $r^2 = 0.36$; Grouped LMI: $\log(\text{MDS}) = -1.17 + 1.98\log(\text{DC})$, $r^2 = 0.42$. Grouped LMI differ from solitary LMI and solitary HMI in slope and intercept ($P < 0.01$).



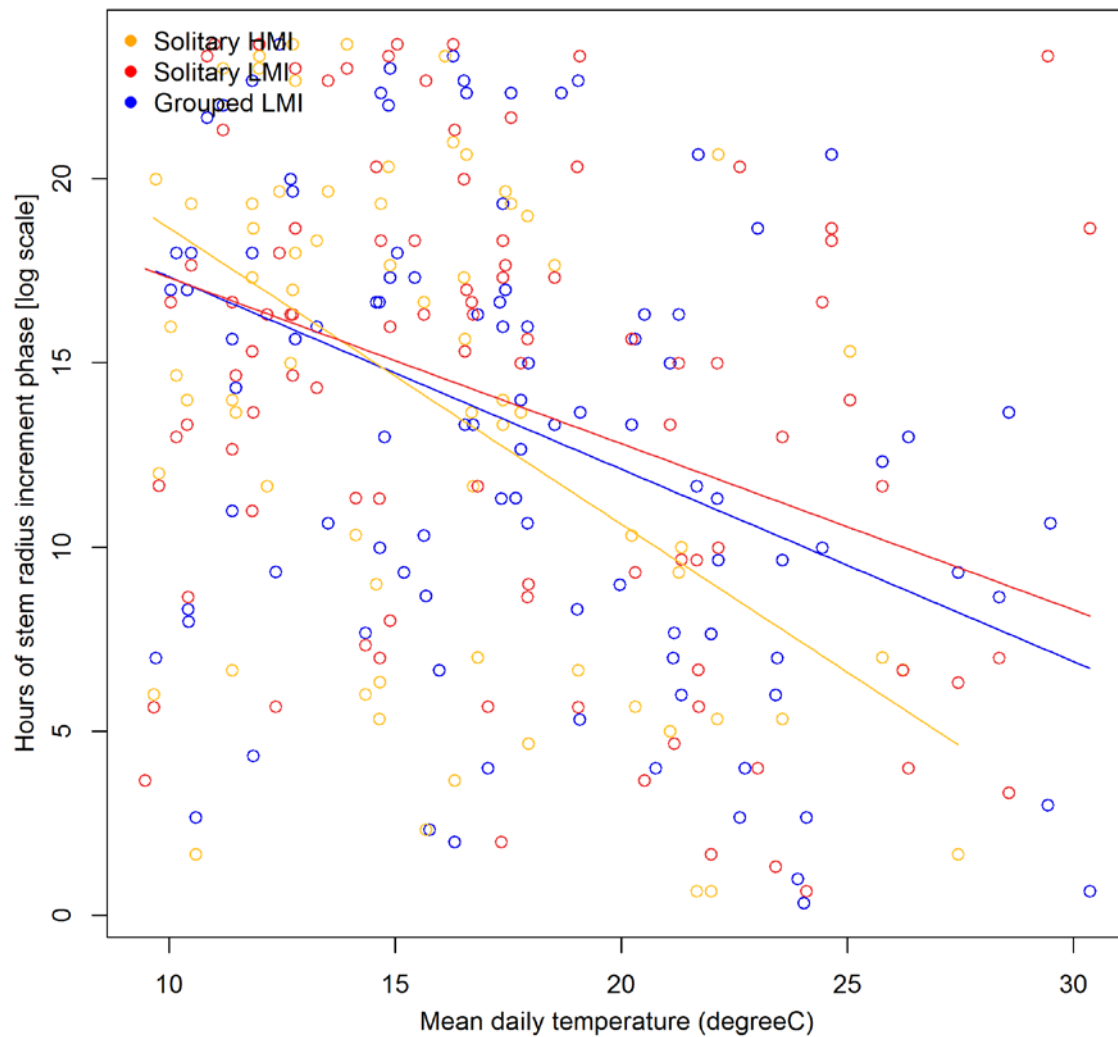
Electronic Appendix 15. Relationship between daily net stem radius increment (ΔR) and the mean daily soil water content (SM). The data were calculated from diurnal cycles in the period April–October 2013. ΔR was calculated when the stem radius exceeded the morning maximum until the subsequent maximum. Solitary LMI: $\log(\Delta R) = -0.04 + 0.05(\text{SM})$, $r^2 = 0.08$, $P < 0.005$; Solitary HMI: $\log(\Delta R) = -0.48 + 3.70\log(\text{SM})$, $r^2 = 0.06$, $P < 0.06$; Grouped LMI: $\log(\Delta R) = -0.53 + 0.06(\text{SM})$, $r^2 = 0.13$, $P < 0.001$. There were non significant pair-wise differences in the slopes of regression lines, and significant differences between solitary LMI and grouped LMI oak in the intercept ($P < 0.01$).



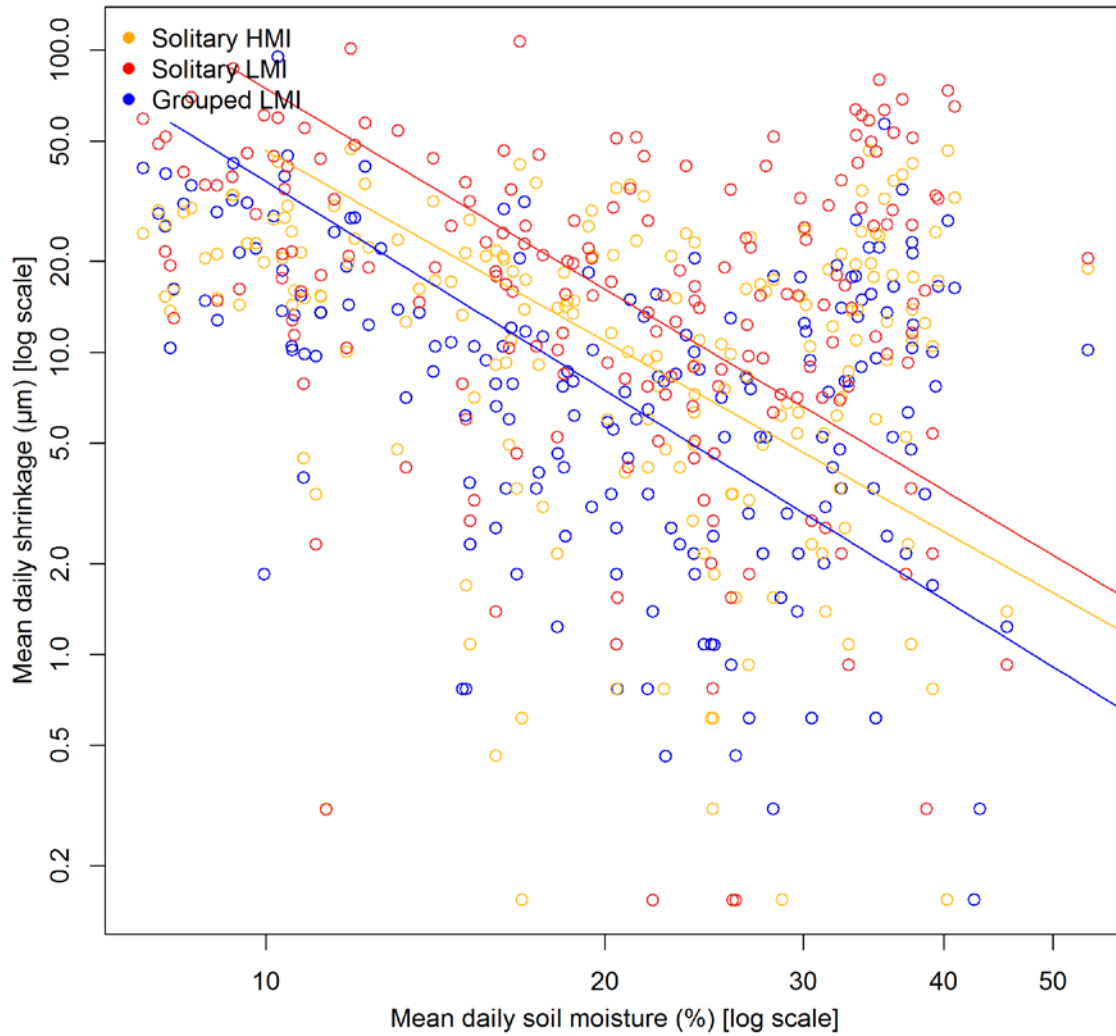
Electronic Appendix 16. Relationship between daily net stem radius increment ($\square R$) and the mean daily air temperature (T). The data were calculated from diurnal cycles in the period April–October 2013. $\square R$ was calculated when the stem radius exceeded the morning maximum until the subsequent maximum. Solitary LMI: $\log(\square R) = 3.37 - 0.11(T)$, $r^2 = 0.08$, $P = 0.005$; Solitary HMI: $\log(\square R) = 3.57 - 0.15(T)$, $r^2 = 0.05$, $P = 0.04$; Grouped LMI: $\log(\square R) = 3.37 - 0.13(T)$, $r^2 = 0.08$, $P = 0.002$. There were nonsignificant pair-wise differences in the slopes of regression lines, and significant differences between solitary LMI and solitary HMI in the intercept ($P < 0.01$). After controlling for the effect of the SRI on $\square R$ in multivariate regressions, daily T had no significant effect on $\square R$ ($P > 0.05$).



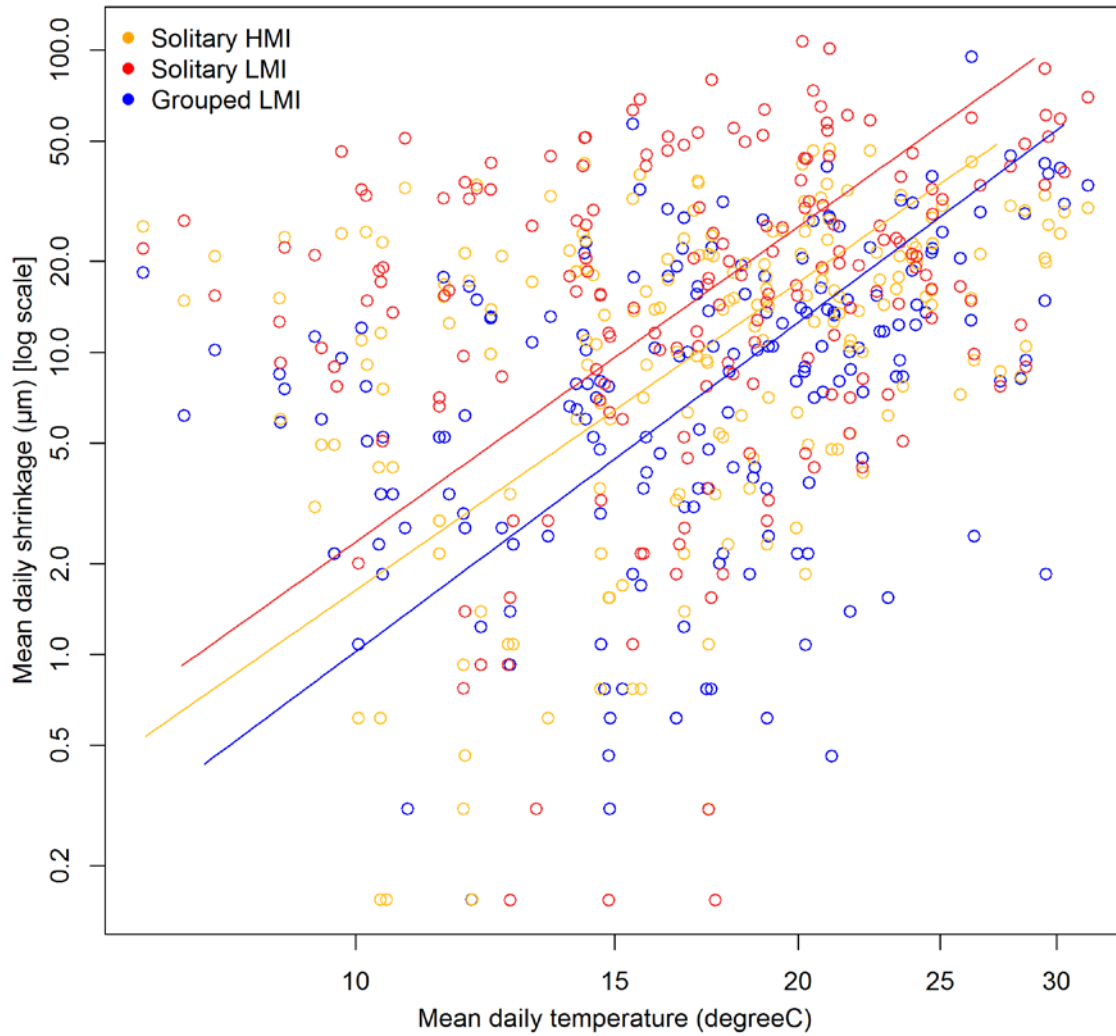
Electronic Appendix 17. Relationship between the duration of stem radius increment phase (SRI) and the mean daily soil water content (SM). The data were calculated from diurnal cycles in the period April–October 2013. Solitary LMI: $SRI = 13.1 + 0.03(SM)$, $r^2 = 0.01$, $P = 0.3$; Solitary HMI: $SRI = 9.88 + 0.15(SM)$, $r^2 = 0.04$, $P = 0.09$; Grouped LMI: $SRI = 7.23 + 0.23(SM)$, $r^2 = 0.12$, $P < 0.001$.



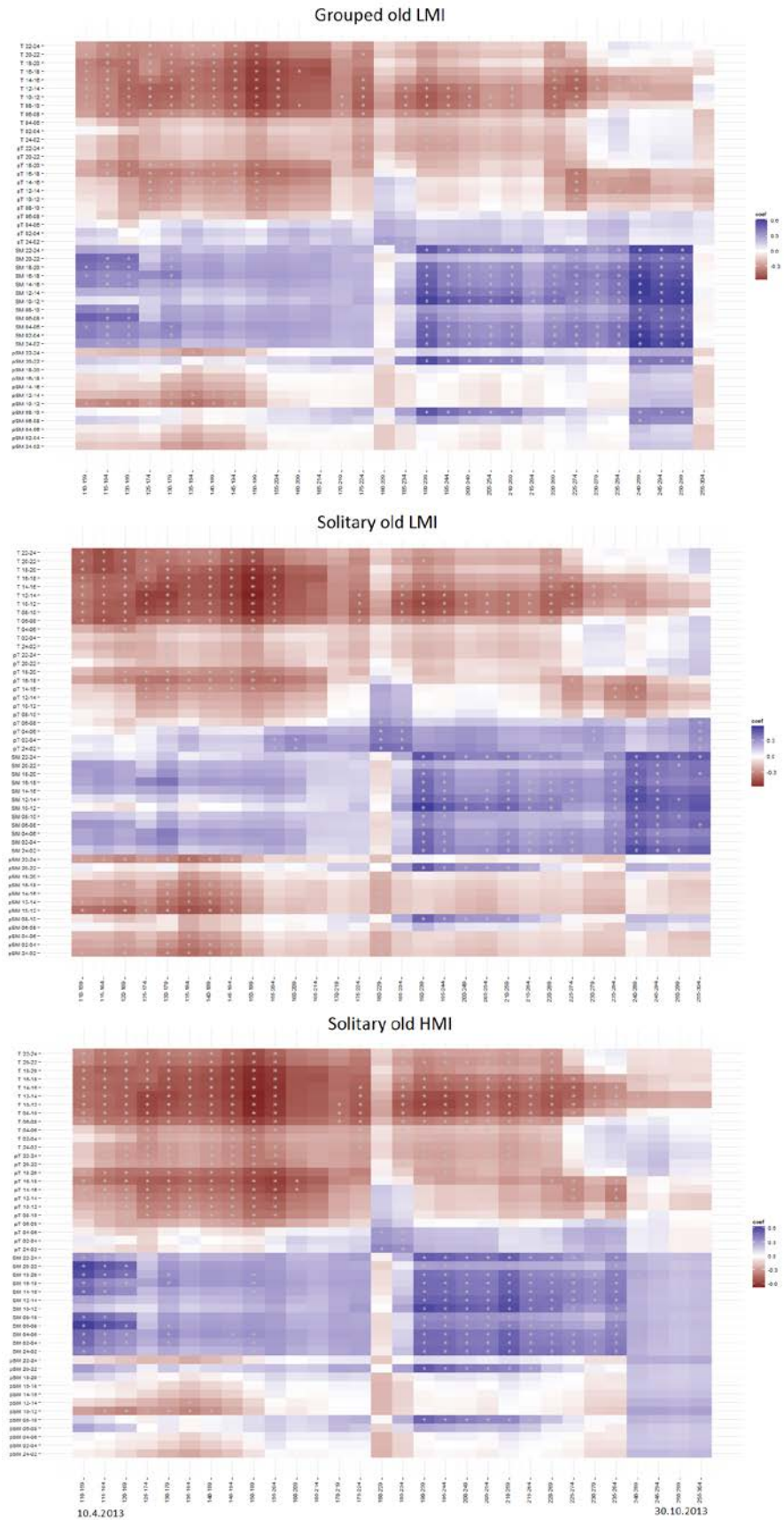
Electronic Appendix 18. Relationship between the duration of stem radius increment phase (SRI) and the mean daily air temperature (T). The data were calculated from diurnal cycles in the period April–October 2013. Solitary LMI: $SRI = 21.8 - 0.45(T)$, $r^2 = 0.08$, $P = 0.003$; Solitary HMI: $SRI = 26.6 - 0.80(T)$, $r^2 = 0.20$, $P < 0.001$; Grouped LMI: $SRI = 22.5 - 0.52(T)$, $r^2 = 0.14$, $P < 0.001$. There were nonsignificant pair-wise differences in the slopes and intercepts of regression lines.



Electronic Appendix 19. Relationship between maximum daily shrinkage (MDS) and the mean daily soil water content (SM). The data were calculated from diurnal cycles in the period April–October 2013. Solitary LMI: $\log(\text{MDS}) = 4.08 - 2.21\log(\text{SM})$, $r^2 = 0.04$, $P = 0.006$; Solitary HMI: $\log(\text{MDS}) = 3.75 - 2.09\log(\text{SM})$, $r^2 = 0.05$, $P = 0.001$; Grouped LMI: $\log(\text{MDS}) = 3.86 - 2.29\log(\text{SM})$, $r^2 = 0.13$, $P < 0.001$. There were significant pair-wise differences in intercepts of regression lines and nonsignificant differences in the slopes.



Electronic Appendix 20. Relationship between maximum daily shrinkage (MDS) and the mean daily air temperature (T). The data were calculated from diurnal cycles in the period April–October 2013. Solitary LMI: $\log(\text{MDS}) = -3.09 + 3.46\log(T)$, $r^2 = 0.05$, $P = 0.001$; Solitary HMI: $\log(\text{MDS}) = -3.16 + 3.38\log(T)$, $r^2 = 0.11$, $P < 0.001$; Grouped LMI: $\log(\text{MDS}) = -3.61 + 3.61\log(T)$, $r^2 = 0.13$, $P < 0.001$. There were significant pair-wise differences in intercepts of regression lines.



Electronic Appendix 21. Bootstrapped moving correlation function relating daily net stem radius increment (ΔR) of solitary HMI oak, and solitary and grouped LMI oaks to in-situ recorded air temperature (T) and soil water content (SM) over the 2013 growing season from April to October. The daily climate data were averaged

by 2-hour intervals and the moving correlations were performed analogously as for annual ring increments and monthly climate data. The moving correlation is carried out in windows of 49 days, offset by 5 days. The blue areas correspond to the positive values and the red areas to the negative ones. Significant correlations are denoted by asterisks. The abbreviated previous-day T and SM are preceded with *p*.